Micropower Class AB Low-Pass Analog Filter Based on the Super-Source Follower

Maite Martincorena-Arraiza, *Student Member, IEEE*, Carlos A. De La Cruz-Blas, *Senior Member, IEEE*, Antonio Lopez-Martin, *Senior Member, IEEE* and Alfonso Carlosena, *Senior Member, IEEE*

***Abstract*— An improved class AB version of the super source follower is used to implement a compact and power-efficient second order analog low-pass filter. The proposed circuit achieves a 41% power reduction as well as an improvement in linearity and pass band gain with respect to its class A counterpart. Measurement results of a test chip prototype fabricated in a 180 nm CMOS technology show a power consumption ranging from 50.3 µW to 85.27 µW for cutoff frequencies from 600 kHz to 890 kHz, with a supply voltage of ±0.75 V. A third order intermodulation distortion of -35.34 dB (for an input signal of 0.4 mV_{pp} and 350 kHz) and a THD of -69.7 dB (for an input signal of 0.4 mV_{pp} and 100 kHz) are measured, which results in an improvement with respect to the conventional class A version of 13.98 dB and 43.6 dB, respectively. The silicon area is 0.0592 mm^2 (using external capacitors).**

***Index Terms*—Analog filter, low-pass filter, class AB, super source-follower, voltage follower, analog CMOS circuits, low-power, quasi-floating-gate MOSFET**

I. Introduction

ADVANCES in portable systems pose new challenges for analog integrated circuit design. Modern designs must trade off features such as circuit simplicity, power consumption, linearity, bandwidth, integration level, noise and offset.

Particularly, analog filters are key elements in many mixed-signal front ends for analog signal processing, with the purpose to reject out-of-band noise and interference. It is difficult to preserve performance of these filters in today's mostly digital integrated circuits, where the power budget for analog circuits is more and more limited.

Active-RC filters with operational amplifiers [1][2][3][4] have been widely used for this purpose, since they achieve large linearity and dynamic range. However, they need passive resistors and power consumption is too large for low-power low-voltage integrated circuits. As an alternative, Gm-C filters [5][6][7] operate in open loop, offering lower power consumption at the expense of reduced linearity. In order to further reduce area and power consumption, alternatives based on simple voltage followers and including capacitors to implement the required poles have been reported [8][9][10][11][12][13]. Thus, techniques using Source Followers (SF) [8] have been proposed due to their low number of internal nodes, as well as power and noise efficiency. However, the SF-C filter in [8], is not adequate for low supply voltages. Alternative approaches employing super source follower (SSF) and Flipped Voltage Follower (FVF) circuits are reported in [9] and [10],[11], respectively. A complementary SF-C low-pass filter for wearable biomedical applications was proposed in [12] that uses a bulk common-mode feedback circuit to stabilize the output level. Finally, [13] uses a current-reuse buffer to design a biomedical low-pass filter.

A limitation of these previous follower-based filters is that the voltage followers operate in class A, i.e., the maximum current that the follower can source or sink is limited by the bias current. This fact can lead to a limited power efficiency, since the bias current must be chosen large enough to achieve the required dynamic range in the worst case. For instance, in channel selection filters a large bias current is often selected to handle large interferers that occur occasionally. Hence the bias current is larger than required for the target dynamic range most of the time. A possible solution is employing class AB voltage followers, so that their dynamic output current is not limited by the bias current. This way, low quiescent power consumption can be achieved preserving at the same time the dynamic performance.

This brief proposes a class AB alternative to the SSF based filter proposed in [9], improving linearity with a simple implementation that preserves the dynamic performance without penalty in static power, noise and area. The brief is organized as follows: In Section II the proposed circuit is described. Section III introduces measurement results of a 180 nm CMOS test chip prototype. Conclusions are drawn in Section IV.

II. Circuit Description

The class A SSF biquadratic cell reported in [9] is shown in Fig. 1(a). The transfer function, natural frequency and quality factor of the circuit in Fig. 1(a) are [9]:

$$H(s)=\frac{1}{1+s\frac{C_1}{g_{m1}}+s^2\frac{C_1C_2}{g_{m1}g_{m2}}};\ w_n=\sqrt{\frac{g_{m1}g_{m2}}{C_1C_2}};\ Q=\sqrt{\frac{C_2}{C_1}\frac{g_{m1}}{g_{m2}}} \quad (1)$$

with g_{mi} the transconductance of transistor M_i. Based on the biquad of Fig. 1(a), the proposed class AB filter is shown in Fig. 1(b). It consists in including a pseudo-resistor with a large-valued resistance R_{large} and a capacitor C_{bat}. This way, node B becomes a Quasi-Floating Gate (QFG) node [14][15], connected to dc bias voltage V_{bp} through the pseudo-resistor, and to node A through capacitor C_{bat}. Under static conditions, capacitor C_{bat} can be considered an open circuit, so the voltage at node B will be equal to bias voltage V_{bp}. Thus, the current across M_4 is controlled by a current mirror and is independent of supply voltage, thermal and process variations, like in the class A version of

Manuscript received.. This work was supported by Grant PID2019-107258RB-C32 funded by MCIN/AEI/10.13039/501100011033. M. Martincorena-Arraiza is funded by the Ministry of Universities under grant BES-2017-080418.

The authors are with the Institute of Smart Cities, Public University of Navarre, E-31006 Pamplona, Spain (e-mail: maite.martincorena@unavarra.es).

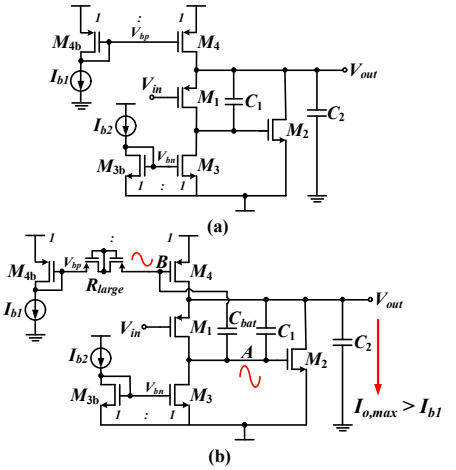

Fig. 1. (a) SSF based-filter (b) Proposed Class AB SSF-based filter.

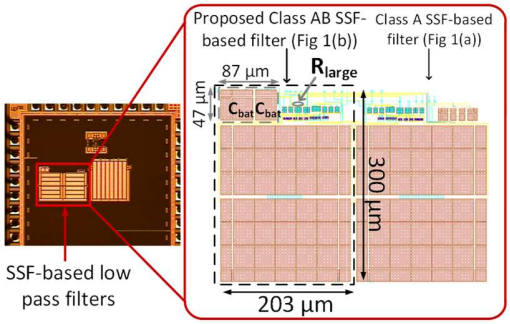

Fig. 2. Fabricated chip. An opaque passivation layer was applied on top of IC. Thus, only capacitors are discernible in the chip photo (on the left). At the right, there is a zoom area with the layout.

Fig. 1(a). However, under dynamic conditions, capacitor C_{bat} acts as a floating battery transferring ac variations from node A to node B with an attenuation equivalent to $\alpha = C_{bat}/(C_{G4} + C_{bat})$, where C_{G4} is the parasitic capacitance at the gate of M_4. If there is an increase in the input voltage, $V_{in,}$ this results in an equivalent decrease in the gate voltage of M_2, which is transferred to the gate of M_4 through C_{bat} increasing its V_{SG} accordingly. This increase allows the drain current of M_4 to be larger than the bias current, resulting in an increase of output current. At the same time, the mentioned decrease in the gate voltage of M_2 decreases its drain current, contributing to a further increase in the output current.

Equation (2) shows the transfer function of the circuit (neglecting body effect), the natural frequency and quality factor of the proposed class AB second order filter.

$$H(s) = \frac{1}{1 + s\frac{C_1}{g_{m1}} + s^2\frac{C_1C_2}{g_{m1}(g_{m2}+\alpha g_{m4})}}$$
$$w_n = \sqrt{\frac{g_{m1}(g_{m2}+\alpha g_{m4})}{C_1C_2}};\ Q = \sqrt{\frac{C_2}{C_1}\frac{g_{m1}}{g_{m2}+\alpha g_{m4}}} \quad (2)$$

Comparing to [9], it can be seen that the QFG technique increases the transconductance of the SSF output branch from g_{m2} to $g_{m2} + \alpha g_{m4}$, since M4 is not just a current source as in Fig. 1(a), but it contributes to the output transconductance. This fact slightly modifies the transfer function, leading to an improvement in the bandwidth of the filter versus Fig. 1(a) for the same bias currents. These expected improvements will be confirmed by the experimental results in Section III. The extra transconductance of the output stage also reduces the output resistance of the filter, which is:

$$R_{out} \approx \frac{1}{g_{m1}[g_{m2} + \alpha g_{m4}]r_{o1}} \quad (3)$$

with r_{o1} the output resistance of M_1.

Another advantage of the proposed biquad cell is the dc gain, which is closer to 0 dB thanks to the extra term αg_{m4}. From (2), the resulting small-signal dc gain of the proposed filter is:

$$A_{DC} = \frac{1}{1 + \frac{1}{g_{m1}r_{o1}} + \frac{1}{g_{m1}[g_{m2}+\alpha g_{m4}](r_{o1}||r_{o3})(r_{o2}||r_{o4}))}} \quad (4)$$

Concerning the noise of the filter, since the measured corner frequency is 80 Hz, at the expected operating frequencies the effects of flicker noise can be neglected, so only thermal noise is considered. In this way, the equivalent input noise power density can be calculated as follows

$$\overline{v_{n,in}{}^2(f)} = 4k_BT\gamma\left[\frac{1}{g_{m1}} + \frac{1}{g_{m2}[g_{m1}(r_{o1}||r_{o3})]^2} + \frac{g_{m3}}{g_{m1}{}^2} + \frac{g_{m4}}{[g_{m1}(g_{m2}+\alpha g_{m4})(r_{o1}||r_{o3})]^2}\right] \quad (5)$$

where k_B is the Boltzmann constant, T the absolute temperature and γ a coefficient equal to 1/3 in weak inversion and 2/3 in strong inversion. It can be observed that the noise contribution of input transistor M_1 dominates, so increasing g_{m1} is highly beneficial. Comparing to the noise expression in [9], the difference is the extra term αg_{m4}, but the improvement versus the class A cell is negligible due to the small value of the last term in (5).

Note that the proposed biquad shows the aforementioned advantages vs Fig. 1(a) for the same power consumption and supply voltage requirements, by simply adding a pseudo-resistor and a capacitor. The only disadvantage is the extra area required for C_{bat}, which is small as described below.

III. Measurement Results

A class AB second order pseudo-differential filter using two matched cells as in Fig. 1(b) was fabricated in a standard 180 nm CMOS technology. The advantage of this arrangement is the avoidance of CMFB circuits, improving power efficiency. The dimensions of the transistors forming the SSF filter cell in Fig. 1(b) are 30µm/0.36µm for M_1 and M_4 and 10µm/0.36µm for M_2 and M_3. The values of the capacitances are C_1 = 15 pF, C_2 = 100 pF and C_{bat} = 1 pF. Currents I_{b1} and I_{b2} are introduced through cascode current mirrors in both positive and negative filter sections from the same current source. Supply voltage was 1.5V. A conventional class A pseudo-differential filter arrangement using two circuits as in Fig. 1(a) was also fabricated on the same chip. For a fair comparison, transistor dimensions, supply voltage and bias currents were the same for both class A and class AB SSF filters. A microphotograph of the two filters is shown in Fig. 2. The proposed circuit occupies an area of 0.0592 mm^2 with external load capacitors (C_2), which means a modest 8.29% area increase with respect to the class A circuit.

Measurements have been obtained using an HP 89440A dynamic signal analyzer, together with an Agilent 33522A signal source. Since the filter's bandwidth is tunable through bias current I_{b1}, maintaining I_{b2} = 10 µA, two different cases have been considered: one with I_{b1}= 20 µA and another with I_{b1}= 10 µA as an extreme case to better show the improvements obtained with the proposed class AB SSF filter. Fig. 3 shows the measured magnitude response of the fabricated class A filter compared with the proposed class AB one for I_{b1} = 20 µA and 10 µA. With

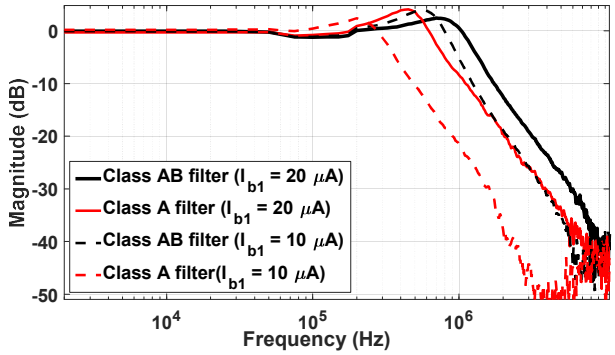

Fig. 3. Measured magnitude response of the filters with and without QFG for a reference bias current I_{b1} of 20 µA and (b) 10 µA.

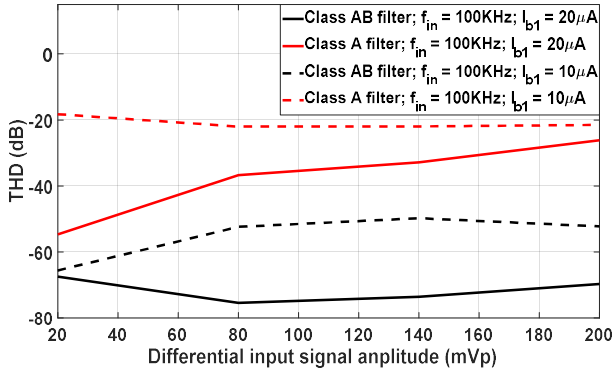

Fig. 4. Measured THD values of the class A and class AB SSF filters for an input signal of 100 kHz and different amplitude values for a reference bias current I_{b1} of (a) 20 µA and (b) 10 µA.

I_{b1} = 20 µA, the cutoff frequency of the class AB filter is 890 kHz, almost a twofold increase with respect to the class A version of 450 kHz in the same bias conditions. A 1000 sample Monte Carlo analysis shows a BW variation of only 1.94%. Moreover, an improvement in linearity is also obtained, as can be seen in Fig. 4 (solid lines) which plots the measured THD at 100 kHz for different input amplitudes. Note that a THD of -69.7 dB is measured for the class AB filter compared to a THD of -26.1 dB for the class A filter, for an input signal of 0.4 mV_{pp}.

On the other hand, setting I_{b1} to 10 µA, Fig. 2 shows a cutoff frequency of 600 kHz for the class AB filter versus 220 kHz for the class A version, an almost threefold increase, under the same bias conditions. The THD values for this extreme case are represented in Fig. 4 (dashed lines). The class AB filter has a THD of -52.25 dB, while the class A filter only reaches a THD of -21.5 dB for a differential input signal of 100 kHz and 0.4 mV_{pp} Low THD values for the class A filter are mainly due to slew rate limitations since the maximum output current is I_{b1}, hence degradation is stronger for smaller I_{b1} as seen in Fig. 4. The class AB version avoids this output current limitation, notably improving THD.

The third order intermodulation distortion has also been analyzed and measured for bias currents of 20 µA and 10 µA to push the circuit to its bias limits and see how the class AB version performs as compared to the conventional class A version. Two frequency ranges have been analyzed; centering the two tones around 50 kHz and 350 kHz. The results for differential input tones of 0.4 V_{pp} can be seen in Fig. 5. Fig. 5(a) shows the IM3 of the class A and class AB filters in both frequency ranges with I_{b1} = 20 µA. With two input tones around 350 kHz the resulting IM3 is -35.34 dB for the class AB version, which is

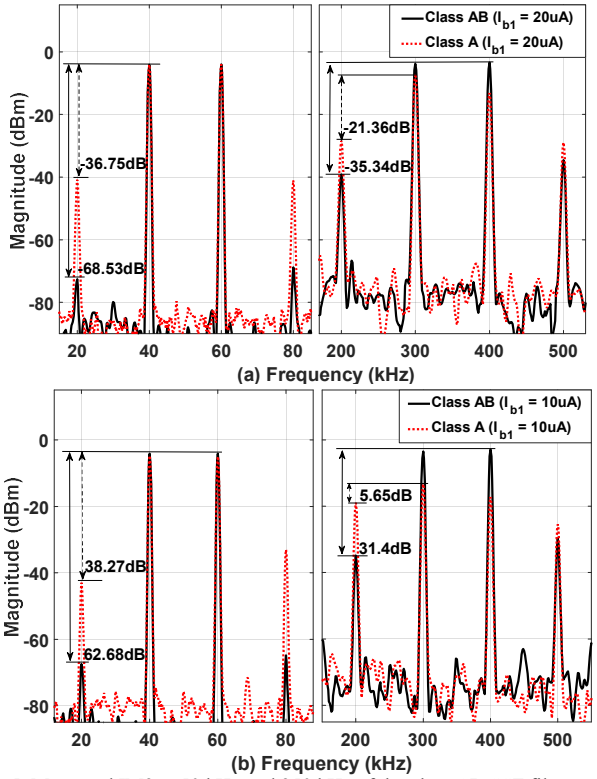

Fig. 5. Measured IM3 at 50 kHz and 350 kHz of the class AB SSF filter (straight line) and class A SSF filter (dotted line) for a reference bias current I_{b1} of (a) 20 µA and (b) 10 µA.

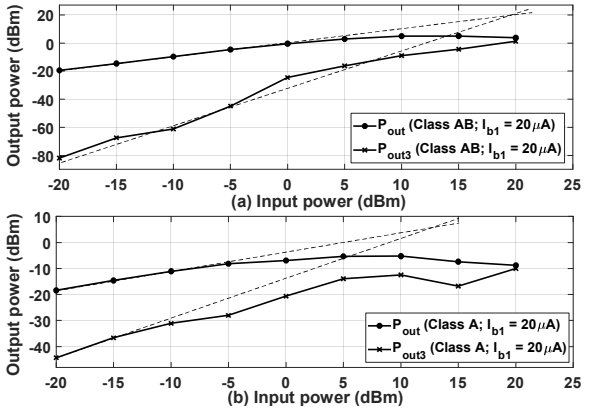

Fig. 6. Measured IP3 at 350 kHz with I_{b1} = 20 µA for (a) the class AB SSF filter (IIP3 = 18 dBm; OIP3 = 20 dBm) and (b) the class A SSF filter (IIP3 = 13 dBm; OIP3 = 5.5 dBm)

13.98 dB larger than that of the class A version. In the 50 kHz range the IM3 of the class AB filter decreases considerably to -68.53 dB, while the class A version experiences a more moderate decrease achieving a IM3 of -36.75 dB. This result shows an improvement of 31.78 dB for this frequency range with the proposed class AB version of the filter. For a bias current of I_{b1} = 10 µA (see Fig. 5(b)), the difference in the 350 kHz range is even higher than with I_{b1} = 20 µA (25.75 dB). This is because, in this scenario, as it can be seen in Fig. 3, the BW of the class A version is reduced to 220 kHz and, therefore, contrary to the class AB version, both tones fall outside the passband of the filter. In this case, the 50 kHz frequency range offers a fairer comparison, where, with an in-band IM3 of -62.68 dB, the class AB filter still renders an IM3 24.41 dB's larger than the class A version. When the input tones are increased to 1 V_{pp}, for the

TABLE I
MAIN MEASURED CHARACTERISTICS OF THE PROPOSED FILTER AND PERFORMANCE COMPARISON

Parameter	This work	Fig.1(a)	[2]	[4]	[8]	[9]	[10]	[12]	[13]
Topology	Class AB SSF-C	Class A SSF-C	Active-RC	Active-RC	SF-C	SSF-C	FVF-C	SF-C	Buffer-C
Order	2nd	2nd	3rd	4th	4th	4th	4th	4th	4th
CMOS Tech.	0.18 µm	0.18 µm	0.13 µm	0.18 µm	0.18 µm	0.18 µm	0.35 µm	0.18 µm	0.35 µm
Supply voltage	1.5 V	1.5 V	1 V	1.8 V	1.8 V	1.8 V	0.6 V	0.5 V	0.9 V
DC gain	-0.04 dB, -0.094 dB	-0.22 dB, -0.26 dB	-	10 dB	-3.5 dB	-2 dB	-2.77 dB	-5.6 dB	-0.03 dB
Bandwidth	600 kHz , 890 kHz	220 kHz , 450 kHz	1 – 20 MHz	600 kHz	10 MHz	33 MHz	101 Hz	200 Hz	101 Hz
IRN	118 nV/$\sqrt{Hz}$	118 nV/$\sqrt{Hz}$	52-85 nV/$\sqrt{Hz}$	126 nV/$\sqrt{Hz}$	7.5 nV/$\sqrt{Hz}$	8 nV/$\sqrt{Hz}$	-	-	-
In-Band integrated Noise	91.4 µVrms , 111.3 µVrms	55.3 µVrms, 79.2 µVrms	-	-	24 µVrms	45 µVrms	46.27 µVrms	91.9 µVrms	80.5 µVrms
THD	-52.25 dB ,-69.7 dB @100kHz&0.4V_{pp}	-26.1 dB, -21.5 dB @100KHz&0.4V_{pp}	-40 dB @300KHz &0.89V_{pp}	-	- 40 dB@3MHz &0.6 V_{pp}	-40 dB @5MHz& 0.55V_{pp}	-40.5 dB @100Hz &0.13 V_{pp}	-40 dB @50Hz&0 .24V_{pp}	-40 dB @100Hz& 0.07V_{pp}
IM3	-35.34 dB @350kHz&0.4V_{pp}	-21.36 dB @350kHz&0.4V_{pp}	-	-	-47 dB @3.5MHz& 0.2V_{pp}	-50 dB @3.5MHz& 0.2V_{pp}	-40 dB @55Hz& 0.048V_{pp}	-40 dB @55Hz& 0.107V_{pp}	-40 dB @55Hz& 0.048V_{pp}
IIP3	18 dBm - 28.5 dBm	13 dBm - 20 dBm	26 dBm, 31.3 dBm	-	17.5 dBm	1dBm, 18 dBm	0.7103 dBm	5 dBm	2 dBm
Power	50.3 µW, 85.27 µW	50.3 µW, 85.27 µW	3-7.5 mW	0.5 mW	4.1 mW	1.38 mW	0.9 nW	3.69 nW	4.26 nW
Die Area	0.0592 mm² *	0.0547 mm² *	1.53 mm²	0.13 mm²	0.52 mm²	0.14 mm²	0.13 mm²	0.075 mm²	0.11 mm²
FoM1	159.24 – 166.24 **	152.9 – 157.6 **	156, 157	158.28	164.4	171.1, 159.73	166	161.85	157
FoM2	149.8 – 154.2 **	144 – 149.42 **	146.1, 149.6	-	157.4	155.9, 156	162	154.86	153

*With external load capacitors (C_2) **@350 kHz (I_{bl} = 20 µm) - @50 kHz (I_{bl} = 20 µm)

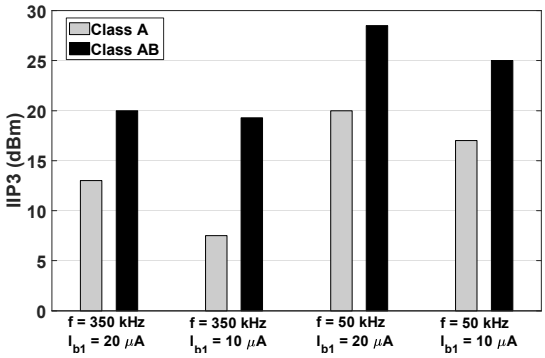

Fig. 7. Comparison of IP3 values in different frequency ranges and bias conditions between the class A SSF filter and the proposed class AB SSF filter.

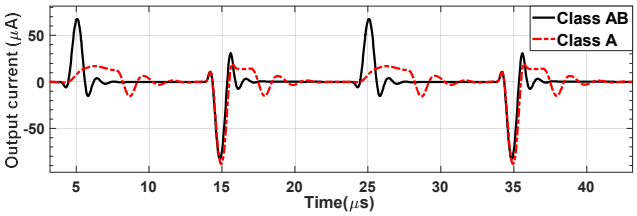

Fig. 8. Measured output current of the proposed class AB filter and its class A counterpart to a 50 kHz square input signal.

proposed class AB filter, IM3 = -20.5 dB (I_{b1} = 20 µA)/-19.8 dB (I_{b1} = 10 µA) at 350 kHz and IM3 = -22.82 dB (I_{b1} = 20 µA)/-23.2 dB (I_{b1} = 10 µA) at 50 kHz.

The third order intercept point (IP3) has been derived from IM3 measurements for different input power levels. Fig. 6 shows the IP3 extracted from the IM3 measurements around 350 kHz with I_{bl}=20 µA. Additionally, for a deeper insight in the linearity improvements of the proposed class AB filter, Fig. 7 shows a comparison between the class A and class AB filter's IP3 performance for both frequency ranges and bias conditions. It can be observed that, in all cases, a larger IP3 is obtained with the class AB filter when compared to the class A version. Particularly, in the case when I_{bl} = 10 µA, there is a notable increment of 12 dB in the frequency range around 350 kHz and of 8 dB in the frequency range around 50 kHz. This improvement in linearity is again due to a better dynamic behavior in class AB operation, which avoids output currents being limited by the bias current. This mitigates slew-rate limitation of linearity as in other class AB filters [16].

Finally, to further demonstrate the class AB operation of the proposed filter, Fig. 8 shows the measured single-ended output current of both the class A and class AB versions of the filter for a 50 kHz square input voltage signal (I_{b1} = 20 µA and I_{b2} = 10 µA). It can be observed that the proposed class AB filter can source an output current not limited by the bias current, providing more symmetrical positive and negative peak output currents and thus achieving a better dynamic operation than its class A counterpart.

When I_{bl}= 20 µA, the static power consumption of both class A and class AB filters is 85.27 µW. However, looking at Fig. 3, it can be seen that the proposed class AB version gets the same BW as the class A version with half the current. This reduction results in a power consumption of 50.3 µW, that is, a reduction of 41% for the same BW. The measured in-band integrated noise of the filter is 111.3 μV_{rms} for the case BW = 890 kHz and 91.4 μV_{rms} for the case BW = 600 kHz.

Table I summarizes the main characteristics of the proposed class AB SSF filter and its class A version and compares it with previously reported designs of similar filters. Note that the target application and, therefore, frequency range of the proposed filter is only similar to [4] and the rest of proposals are aimed either at very low frequency operation for biomedical applications [10],[12],[13], or at higher frequency standards such as WiFi [2], [8], [9]. For this reason, the fabricated class A version of the filter, based on [9] (Fig. 1(a)) but designed in the same process and for the same frequency range, is a very useful benchmark to highlight the improvements of the proposed filter.

The filter is competitive with previous works in terms of dc gain accuracy, achieving gains very close to unity. The required supply voltage is lower than that of other works employing the same CMOS technology. The main advantage of the proposed filter, mainly due to the use of the QFG technique, is the improvement in linearity, obtaining the lowest THD value at -69.7 dB. Finally, as mentioned before, a 41% reduction of power consumption is obtained when comparing to the fabricated class A SSF filter for the same bandwidth. A much lower power consumption than [4] is obtained for the same frequency ranges.

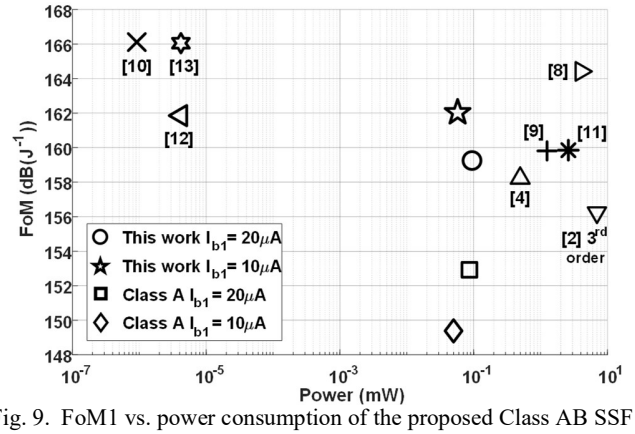

Fig. 9. FoM1 vs. power consumption of the proposed Class AB SSF filter (for bias currents of 10 μA and 20 μA) compared to the fabricated Class A version of the filter and previous works.

A common way to compare the proposed filter to previous works in terms of important parameters such as linearity, noise, bandwidth and power, is by using a Figure-of-Merit (FoM). The following FoMs (here referred as FoM1 and FoM2) are used considering the above-mentioned characteristics [9].

$$FoM1 = 10log_{10}\left(\frac{IMFDR_3 \cdot f_{-3dB} \cdot N}{P_w}\right)$$
$$FoM2 = 10log_{10}\left(\frac{IMFDR_3 \cdot f_{-3dB} \cdot N}{P_w}\right)\left[\frac{f_{IM3L}}{f_{poles}}\right] \quad (6)$$

where P_w is the power consumption of the circuit, f_{-3dB} is the cutoff frequency, N is the order of the filter and $IMFDR_3$ is the spurious-free IM3, which is calculated as follows:

$$IMFDR_3 = \left(\frac{IIP3}{V_{N.in}}\right)^{4/3} \quad (7)$$

$IIP3$ being the third order input intercept point and $V_{N.in}$ the in-band integrated input referred noise. f_{IM3L} is the lower 3rd-order intermodulation tone frequency and f_{poles} the pole frequency.

Fig. 9 shows the FoM1 vs. power consumption of the proposed filter and previous works, considering the IP3 obtained in the frequency band nearest to the cutoff frequency of each filter (in this case the band around 350 kHz), to compare their performance. Comparing with the fabricated class A version of the SSF filter under the same conditions, an improvement in FoM of around 10 is obtained for each bias current case. Comparing with previous works, it is important to remember that the frequency range of operation is different than that of such previous works. Some operate at frequencies in the range of GHz at the cost of higher power consumption, while others, aimed at biomedical applications work at frequency ranges of a few hundreds Hertz, with a much lower power consumption. Note that the proposal is clearly superior to the class A version and is competitive with state-of-the-art filters, being the only one in Fig. 8 combining tunability and class AB operation.

IV. Conclusions

A novel class AB SSF filter has been proposed, suited for low-power, low-voltage operation. The use of the QFG technique enhances the circuit operation achieving a considerable reduction in power consumption and improvement in linearity, bandwidth and pass band gain. The filter cutoff frequency is also tunable by means of the bias current I_{b1}, resulting in a simple and compact solution suitable for low-power systems, such as low-power channel selection filters for Bluetooth receivers.

References

[1] M. Banu, and Y. Tsividis, "Fully Integrated Active RC Filters in MOS Technology," *IEEE J. Solid-State Circuits*, vol. 18, no. 6, pp. 644–651, 1983, doi: 10.1109/JSSC.1983.1052014.

[2] H. Amir-Aslanzadeh, E. J. Pankratz, and E. Sanchez-Sinencio, "A 1-V +31 dBm IIP3, reconfigurable, continuously tunable, power-adjustable active-RC LPF," *IEEE J. Solid-State Circuits*, vol. 44, no. 2, pp. 495–508, 2009, doi: 10.1109/JSSC.2008.2011037.

[3] W. Wu, T. Mo, and Z. Lu, "A 180nm CMOS three stage feedforward compensation op-amp with linearity improvement technique for active RC LPF," *Proc. 2016 10th IEEE Int. Conf. Anti-Counterf., Secur. Ident., ASID 2016*, pp. 91–95, 2017, doi: 10.1109/ICASID.2016.7873924.

[4] A. Rasekh and M. Sharif Bakhtiar, "Design of Low-Power Low-Area Tunable Active RC Filters," *IEEE Trans. Circuits Syst. II Express Briefs*, vol. 65, no. 1, pp. 6–10, 2017, doi: 10.1109/tcsii.2017.2658635.

[5] C. Yoo, S. Lee, and W. Kim, "Filter with a Single-Integrator Based Tuning," vol. 33, no. 1, pp. 18–27, 1998.

[6] H. Voorman and H. Veenstra, "Tunable High-Frequency Gm-C Filters," vol. 35, no. 8, pp. 1097–1108, 2000.

[7] C. Chanapromma, A. Prajong, S. Adirek, and W. Wattanasin, "High even-order fully-differential biquadratic continuous-time low-pass Gm-C filter," *2014 Int. Electr. Eng. Congr. iEECON 2014*, pp. 1–4, 2014, doi: 10.1109/iEECON.2014.6925853.

[8] S. D'Amico, M. Conta, and A. Baschirotto, "A 4.1-mW 10-MHz fourth-order source-follower-based continuous-time filter with 79-dB DR," *IEEE J. Solid-State Circuits*, vol. 41, no. 12, pp. 2713–2719, 2006, doi: 10.1109/JSSC.2006.884191.

[9] M. De Matteis, A. Pezzotta, S. D'Amico, and A. Baschirotto, "A 33 MHz 70 dB-SNR super-source-follower-based low-pass analog filter," *IEEE J. Solid-State Circuits*, vol. 50, no. 7, pp. 1516–1524, 2015, doi: 10.1109/JSSC.2015.2411626.

[10] C. Sawigun and S. Thanapitak, "A 0.9-nW, 101-Hz, and 46.3- μVrms IRN Low-Pass Filter for ECG Acquisition Using FVF Biquads," vol. 26, no. 11, pp. 2290–2298, 2018.

[11] M. De Matteis and A. Baschirotto, "A biquadratic cell based on the flipped-source-follower circuit," *IEEE Trans. Circuits Syst. II Express Briefs*, vol. 64, no. 8, pp. 867–871, 2017, doi: 10.1109/TCSII.2016.2611061.

[12] Z. Liu, Y. Tan, H. Li, H. Jiang, J. Liu, and H. Liao, "A 0.5-V 3.69-nW Complementary Source-Follower-C Based Low-Pass Filter for Wearable Biomedical Applications," *IEEE Trans. Circuits and Syst. I: Reg. Papers* vol. 67, no. 12, pp. 4370–4381, 2020.

[13] S. Thanapitak and C. Sawigun, "A subthreshold buffer-based biquadratic cell and its application to biopotential filter design," *IEEE Trans. Circuits Syst. I Regul. Pap.*, vol. 65, no. 9, pp. 2774–2783, 2018, doi: 10.1109/ TCSI.2018.2808361.

[14] J. Ramírez-Angulo, A. J. López-Martín, R. González Carvajal, and F. Muñoz Chavero, "Very low-voltage analog signal processing based on quasi-floating gate transistors," *IEEE J. Solid-State Circuits*, vol. 39, no. 3, pp. 434–442, 2004, doi: 10.1109/JSSC.2003.822782.

[15] J. Ramírez-Angulo, C. A. Urquidi, R. González-Carvajal, A. Torralba, and A. López-Martin, "A new family of very low-voltage analog circuits based on quasi-floating-gate transistors," *IEEE Trans. Circuits Syst. II Analog Digit. Signal Process.*, vol. 50, no. 5, pp. 214–220, 2003, doi: 10.1109/TCSII.2003.811434.

[16] C. Garcia-Alberdi, A. J. Lopez-Martin, L. Acosta, R. G. Carvajal and J. Ramirez-Angulo, "Tunable Class AB CMOS Gm-C Filter Based on Quasi-Floating Gate Techniques," *IEEE Transactions on Circuits and Systems I: Regular Papers*, vol. 60, no. 5, pp. 1300-1309, May 2013, doi: 10.1109/TCSI.2012.2220504.